Bulletin of the Seismological Society of America, Vol. 97, No. 1A, pp. S18–S24, January 2007, doi: 10.1785/0120050623

The Energy Radiated by the 26 December 2004 Sumatra–Andaman Earthquake Estimated from 10-Minute *P*-Wave Windows

by George L. Choy and John Boatwright

Abstract The rupture process of the M_W 9.1 Sumatra–Andaman earthquake lasted for approximately 500 sec, nearly twice as long as the teleseismic time windows between the *P* and *PP* arrival times generally used to compute radiated energy. In order to measure the *P* waves radiated by the entire earthquake, we analyze records that extend from the *P*-wave to the *S*-wave arrival times from stations at distances $\Delta > 60°$. These 8- to 10-min windows contain the *PP, PPP*, and *ScP* arrivals, along with other multiply reflected phases. To gauge the effect of including these additional phases, we form the spectral ratio of the source spectrum estimated from extended windows (between T_P and T_S) to the source spectrum estimated from normal windows (between T_P and T_{PP}). The extended windows are analyzed as though they contained only the *P-pP-sP* wave group. We analyze four smaller earthquakes that occurred in the vicinity of the M_W 9.1 mainshock, with similar depths and focal mechanisms. These smaller events range in magnitude from an M_W 6.0 aftershock of 9 January 2005 to the M_W 8.6 Nias earthquake that occurred to the south of the Sumatra–Andaman earthquake on 28 March 2005. We average the spectral ratios for these four events to obtain a frequency-dependent operator for the extended windows. We then correct the source spectrum estimated from the extended records of the 26 December 2004 mainshock to obtain a complete or corrected source spectrum for the entire rupture process (~600 sec) of the great Sumatra–Andaman earthquake. Our estimate of the total seismic energy radiated by this earthquake is 1.4×10^{17} J. When we compare the corrected source spectrum for the entire earthquake to the source spectrum from the first ~250 sec of the rupture process (obtained from normal teleseismic windows), we find that the mainshock radiated much more seismic energy in the first half of the rupture process than in the second half, especially over the period range from 3 sec to 40 sec.

Introduction

In terms of radiated energy, the Sumatra–Andaman earthquake of 26 December 2004 is the largest thrust-fault earthquake to have occurred since the U.S. Geological Survey (USGS) National Earthquake Information Center (NEIC) began routine computation of radiated energy E_S and energy magnitude M_e for teleseismic earthquakes in 1987. The focal parameters for the Sumatra–Andaman earthquake as determined by the NEIC are as follows: origin time (OT) 26 December 2004, 00:58:53.4 coordinated universal time (UTC), 3.295°N, 95.982°E, M_W 9.1, M_e 8.5. The rupture characteristics of this earthquake have been summarized by Bilham (2005), Lay *et al.* (2005), and Ammon *et al.* (2005). As befitting a megathrust earthquake of M_W 9.1, the rupture length of the earthquake was at least 1200 km. The duration of the rupture process was commensurately long. Indeed, the duration, as constrained by several studies of bandlimited data, far exceeded that of any earthquake encountered to date. Lomax (2005) and Krüger and Ohrnberger (2005) exploit the fact that later arrivals (primarily *PP* and *PPP*) are depleted of high-frequency energy by virtue of ray paths that propagate multiple times in an attenuating upper mantle. After high-pass filtering of seismic records the decay of the *P*-wave signal can be easily seen. Ishii *et al.* (2005), by using directional stacking of short-period data from Hi-Net, a dense seismic array in Japan, were able to isolate the *P* wave. The consensus among these analyses is that the preponderance of the moment and energy release by the rupture process took place in the first 250 sec, with some minor patches of high-frequency release up to 8 min after the onset of *P*. At the other end of the seismic spectrum, several finite-fault inversions (Ammon *et al.*, 2005) using low-frequency surface-wave data derived moment rate functions that had similar durations between 500 and 600 sec. Although the rupture duration can be well estimated with band-limited

data, the computation of radiated energy requires the analysis of a broad bandwidth of data including frequencies above and below the corner frequency of teleseismically recorded earthquakes.

The method used by the USGS for estimating the radiated seismic energy of teleseismic earthquakes is that of Boatwright and Choy (1986) in which the energy flux in broadband *P* waves is obtained by direct integration of velocity-squared records. Velocity-squared spectra of body waves are corrected for effects arising from source mechanism, depth phases, and frequency-dependent propagation through the earth. Similar methods for computing energy have been used by others (e.g., Houston, 1990; Newman and Okal, 1998; Perez-Campos and Beroza, 2001; Venkataraman and Kanamori, 2004). These methods generally employ a time window corresponding to the time interval over which the fault is dynamically rupturing. When broadband data are used, delimiting the time window is generally unequivocal regardless of the complexity of rupture or the size of the earthquake. The initial arrival of energy is obviously identified with the onset of the direct *P* wave. The end of the dynamic rupture process and the point at which radiated energy becomes negligible can be identified where the amplitude of the velocity-squared signal decays to the level of the coda noise. Until the advent of the M_W 9.1 Sumatra–Andaman earthquake, the decay in amplitude of the source duration always occurred before the arrival of the phase *PP*. In the Sumatra–Andaman earthquake we encountered for the first time an earthquake for which the velocity-squared amplitude of the *P* wave did not noticeably decay down to the coda level before the arrival of *PP*.

The purpose of this article is to develop a method that will enable us to extend the use of teleseismic *P* waves to obtain the radiated energy for a megathrust earthquake. The method must account for a *P*-wave rupture duration that overlaps significant secondary phase arrivals. Reliable estimates of E_S are an essential complement to other source parameters characterizing the earthquake. Global studies of the variability of radiated energy with seismic moment M_0 have found that the empirical formulas that estimate E_S from M_0 or M_S are poor predictors of E_S (e.g., Choy and Boatwright, 1995). That earthquakes with the same M_0 can have substantially different E_S has profound consequences for investigating the mechanics of earthquakes as well as for evaluating seismic hazard.

Method of Spectral Analysis

Our methodology starts with finding reference events with short source durations from which we can develop a frequency-dependent operator that accounts for the effect of having included multiply reflected phases in a time window.

We choose four reference events with locations in the vicinity of the rupture zone of the mainshock (Fig. 1, Table 1). Although the length of the rupture of the mainshock ranges from approximately 2° to 13° N (e.g., Ammon *et al.*, 2005), there were no large aftershocks above 8° N that were suitable as additional reference events. However, the moderate variations in strike and dip of the fault along the rupture do not affect our results. As shown in Boatwright and Choy (1986) and by Newman and Okal (1998), the generalized radiation-pattern coefficient used to account for focal mechanism is stable and relatively invariant for predominantly dip-slip earthquakes.

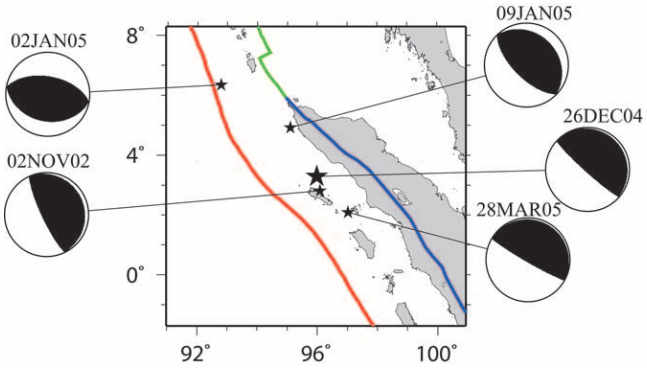

Figure 1. Locations and focal mechanisms of the four reference events and the Sumatra–Andaman earthquake of 26 December 2004.

The range of M_W for the reference events is from 6.0 to 8.6. Their distribution in space about the epicenters of the mainshock will average the variations in ray paths and bounce points in the earth. Two of the events are sizable aftershocks (M_W 6.0 and 6.4). The 2 November 2002 with M_W 7.4 is the largest earthquake since the deployment of global digital seismograph networks to have occurred within 2° of and prior to the mainshock. The largest of our reference events is the M_W 8.6 Nias earthquake of 26 March 2005. The raw data are digital recordings obtained from the Global Seismographic Network (GSN) that are processed using the method of Harvey and Choy (1982) to obtain broadband velocity records. In order to have ~600-sec windows between the onset of the *P* wave and the arrival of the *S* wave, we use records from stations only at distances greater than about 60°. The broadband velocity record for these events at a representative station, MORC, are shown in Figure 2.

For each reference event, the radiated energy using the normal short *P*-wave window (i.e., the record section between T_P and T_{PP} along with presignal and postsignal padding) is computed using the method of Boatwright and Choy (1992). First, an average acceleration spectrum is obtained by logarithmically averaging the acceleration spectra of velocity records (using the normal time window) that have been corrected for frequency-dependent anelastic attenuation and geometric spreading. For broadband data, the attenuation operator must be both frequency dependent and dispersive. An appropriate operator, valid over the broad bandwidth of frequencies analyzed, is given by Choy and Cormier (1986). The average acceleration spectrum is then corrected for the effect of the free surface, that is, spectral

Table 1
Source Parameters of Earthquakes Analyzed in This Study

Date	Latitude (°)	Longitude (°)	m_b	M_S	M_e	M_W	Strike (°)	Dip (°)	Slip (°)
2 November 2002	2.82	96.09	6.2	7.6	7.1	7.4	297	16	73
2 January 2005	6.36	92.79	5.7	6.2	6.0	6.4	338	26	86
9 January 2005	4.93	95.11	6.0	5.8	5.6	6.0	311	22	88
28 March 2005	2.09	97.11	7.2	8.4	8.1	8.6	326	7	106
24 December 2004	3.30	95.98	7.0	8.8	8.5	9.1	327	6	105

The location and magnitudes are those reported by the NEIC. The focal mechanisms are the Harvard CMT solutions (Harvard Seismology, 2006). M_e is energy magnitude where $M_e = (2/3) \log E_S - 2.9$ from Choy and Boatwright (1995). The first four events are the reference events.

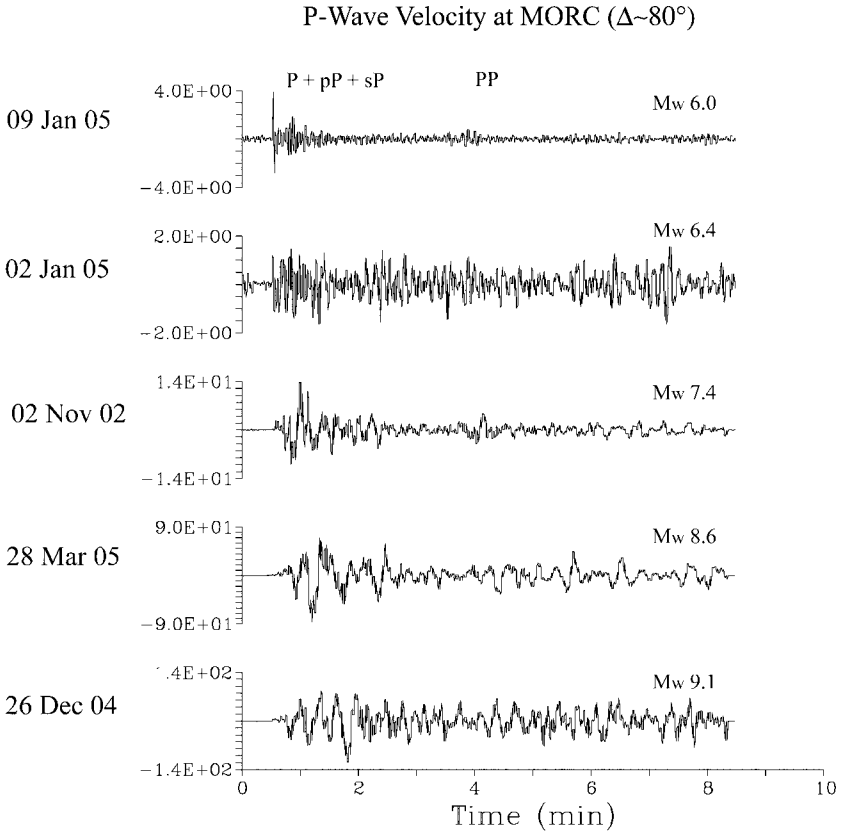

Figure 2. Broadband velocity seismograms at station MORC (Moravsky Beroun, Czech Republic) for the earthquakes of this study. The station is about 80° from the epicentral region of the Sumatra–Andaman earthquake.

modulations caused by the interference of the direct phase and surface reflections (*pP* and *sP* for the *P*-wave group). The resulting spectrum is called the corrected acceleration spectrum of the event. This is shown with 85% confidence limits as the light gray area in Figures 3–6. The E_S values from the spectrum of these short windows are listed in the first column of Table 2.

Next the same procedure is applied to the extended window (i.e., the record section between T_P and T_S) of each event. The data in this second step are still treated as if they contained only the *P*-wave group (consisting of direct *P, pP*, and *sP*). The resulting corrected acceleration spectrum with 85% confidence limits for each event is shown in Figures 3–6 as the dark gray area. The E_S values derived from the spectrum of the extended windows are listed in the second column of Table 2. They are, of course, contaminated by the inclusion of energy from secondary phases such as *PP, PPP*, and *ScP*.

To remove the effect of having included multiply reflected phases within the extended window, a correction operator can be obtained that shapes the spectrum of the extended window $A_{(T_P\text{-}T_S)}$ into the spectrum of the short window $A_{(T_P\text{-}T_{PP})}$. This correction operator is simply the ratio of the amplitude spectrum of the short window to the amplitude spectrum of the extended window. The amplitude ratios as a function of frequency for the reference events are shown as dashed lines in Figure 7. In general, the effect of including *PP, PPP*, and *ScP* arrivals is to enrich amplitudes in the band between 0.03 and 0.3 Hz, although some elevation continues at the high-frequency end.

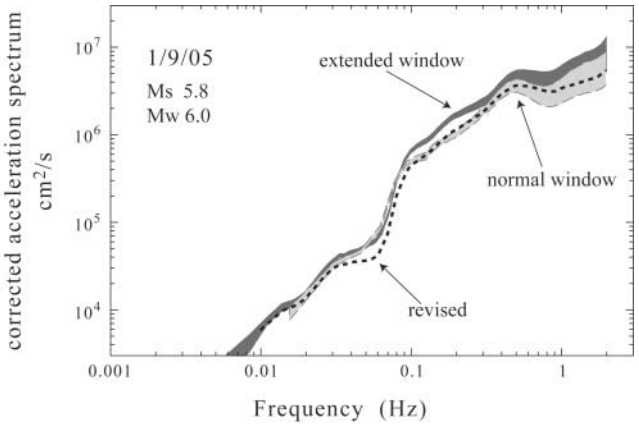

Figure 3. The acceleration spectrum for *P* waves for the extended and normal time windows for the foreshock of 9 January 2005, M_S 5.8. Each spectrum has been corrected for frequency-dependent attenuation, geometric spreading, focal mechanism, and modulation from *pP* and *sP*. The light gray area shows the corrected source spectrum with 85% confidence bounds obtained from the normal short window (taken between T_P and T_{PP}, the arrival times of *P* and *PP*). The dark gray area is similar but shows the corrected source spectrum for the extended window (taken between T_P and T_S, the arrival times of *P* and *S*). The dashed line is the revised acceleration spectrum that results when the correction operator of Figure 7 is applied to the spectrum of the extended window. The revised spectrum is a good fit to the spectrum of the normal short window at intermediate frequencies (0.05–0.5 Hz).

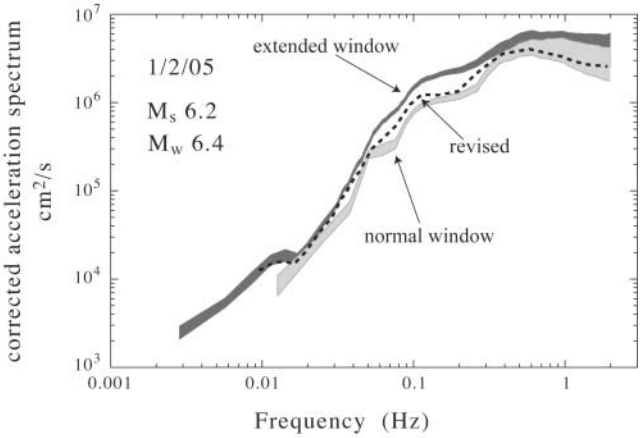

Figure 4. The acceleration spectra for *P* waves for the foreshock of 2 January 2005, M_S 6.2: the extended time window (dark gray curve); the normal short window (light gray); and the revised acceleration spectrum that results when the correction operator is applied to the spectrum of the extended window (dashed curve).

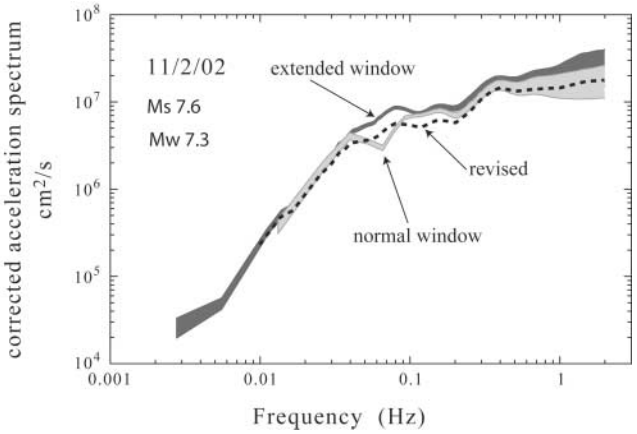

Figure 5. The acceleration spectra for *P* waves for the earthquake of 2 November 2002, M_S 7.6: the corrected source spectrum from the normal short window (light gray); the corrected source spectrum from the extended window (dark gray); and the revised acceleration spectrum (dashed).

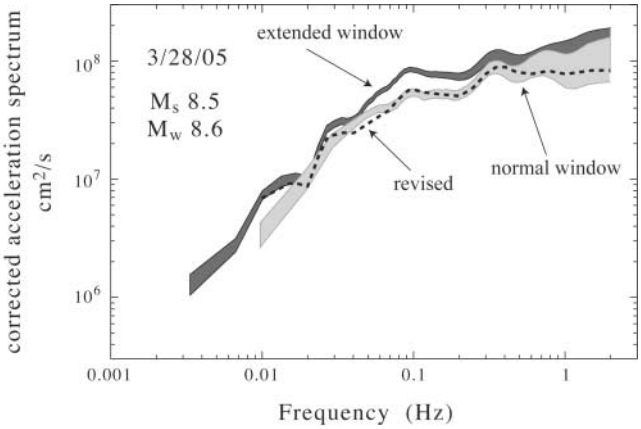

Figure 6. The acceleration spectrum for *P* waves for the earthquake of 28 March 2005, M_S 8.4: the corrected source spectrum obtained from the normal short window (light gray); the corrected source spectrum from the extended window (dark gray); and the revised acceleration spectrum (dashed).

Applying the correction operator for each event to its own extended-window spectrum would trivially return the correct E_S for the short normal window. The mainshock, however, had an extended rupture length of several hundred kilometers. Thus, we take as the correction operator the average of the four operators (solid line in Fig. 7), which serves to average the effect of earth structure about the source region as well as along the propagation paths. To check the effect of this average correction operator, we apply it to rederiving E_S on the smaller events before applying it to the mainshock. The revised spectra obtained by applying the correction operator to the spectra of the extended windows (dashed line in Figs. 3–7) are in fairly good agreement with the spectra from the normal windows for the three smallest

Table 2
The Energies Computed for the Reference Events and the Mainshock Using Spectra from the Normal (Short) Window and the Revised Window (Extended Window after Application of the Correction Operator)

Date	E_S (J) (Short Normal Window)	E_S (J) (Extended Window Revised)	M_0 (N m) (HRV)
2 November 2002	0.7×10^{15}*	1.1×10^{15}	9.0×10^{19}
2 January 2005	2.2×10^{13}*	4.7×10^{13}	4.2×10^{18}
9 January 2005	2.0×10^{13}*	3.0×10^{13}	1.1×10^{18}
28 March 2005	3.7×10^{16}*	3.9×10^{16}	1.1×10^{22}
26 December 2004	0.6×10^{17}	1.3×10^{17}*	4.0×10^{22}

*Preferred E_S values.

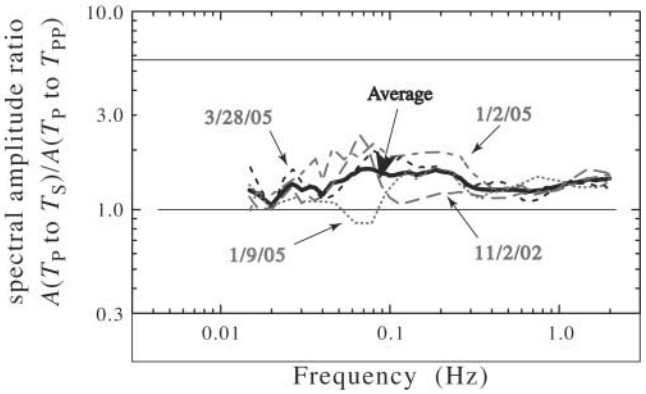

Figure 7. The ratio of the extended-window spectrum to the short-window spectrum, $A_{(T_S\text{-}T_P)}/A_{(T_{PP}\text{-}T_P)}$, for each of the reference events. The average (solid line) is used as the correction operator for the extended-window spectrum of the mainshock.

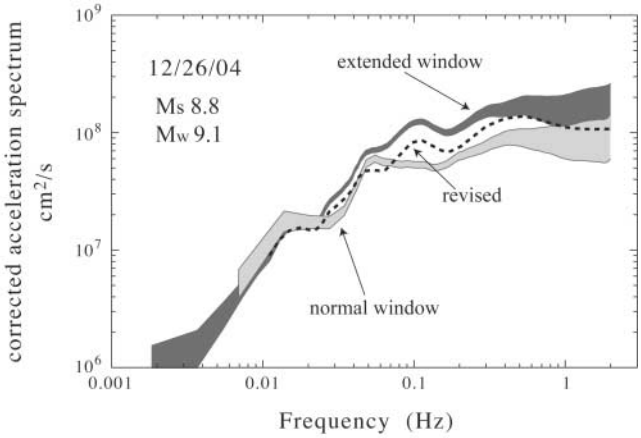

Figure 8. The acceleration spectrum for *P* waves for the extended and normal time windows for the earthquake of Sumatra–Andaman earthquake of 26 December 2004, M_S 8.8. The light gray curve shows the corrected source spectrum obtained from the normal short window. The dark gray curve shows the corrected source spectrum for the extended window. The dashed line is the acceleration spectrum that results when the correction operator is applied to the spectrum of the extended window.

events. The revised spectrum of the largest reference event, the Nias earthquake of 28 March 2005, is in excellent agreement with some amplitude depletion near 0.03 Hz. The E_S values derived from the corrected spectrum of the extended windows are listed in the third column of Table 2.

The results for the Sumatra–Andaman mainshock are shown in Figure 8. For the four reference events, the preferred spectrum for deriving E_S is the normal (short) window. For the Sumatra–Andaman mainshock, the preferred E_S is derived from correcting the spectrum of the extended window. After application of the correction, the resulting E_S for the earthquake is 1.4×10^{17} J. This is in excellent agreement with the E_S 1.2×10^{17} J derived by Singh *et al.* (2005) using broadband records from seismograph stations in India at regional and teleseismic (<45°) distances. Our value is also at the lower bound of E_S ($1.38–2.98 \times 10^{17}$ J) estimated by Kanamori (2006) using a finite rupture model for the moment-rate function for the mainshock. In comparison, the Gutenberg–Richter formulas, which use M_S or M_W to estimate E_S, would have yielded 1.4×10^{18} J and 2.8×10^{18} J, respectively. The empirical formulas appear to substantially overestimate E_S relative to any of the direct estimates.

Discussion

A comparison of the corrected-source spectrum of the extended window (~600 sec) and the source spectrum from the short window (~250 sec) for the Sumatra–Andaman earthquake shows the relative amount of energy radiated as a function of frequency as the rupture progressed (Fig. 8). At frequencies from about 0.07 to 0.7 Hz, the extended-window spectrum exceeds the normal short-window spectrum by 20% to 60%. Thus, the second half of the rupture radiated less high-frequency energy than the first half of the rupture. Our result corresponds with the moment tensor inversions that found most of the moment release in the first 250 sec (see figure 6 of Ammon *et al.*, 2005), but disagrees with Kanamori (2006) who estimates that the second half of the rupture radiated 35% of the total energy (see his fig. 7).

At frequencies from 0.01 to 0.07 Hz, however, the

extended-window and short-window spectra essentially overlie each other, suggesting that the second half of rupture radiated almost no low-frequency energy. Our result corresponds with the deconvolutional analyses of Singh *et al.* (2005) who found that the Indian stations contain almost no low-frequency (0.01 to 0.05 Hz) energy after the initial strong arrivals. This remarkable result suggests the rupture process in the second half of the earthquake is fundamentally different than the rupture process in the first half.

Two asymptotic results constrain almost all models of seismic spectra: the acceleration spectra are flat for high frequencies, while the displacement spectra are flat for periods longer than the overall duration of slip on the fault. In their analysis of the acceleration spectra of a suite of subduction zone earthquakes with M_S from 6.2 to 8.1, Boatwright and Choy (1989) found a discontinuous change in spectral behavior occurring at $M_0 \sim 10^{20}$ N m. The suite of earthquakes of the Sumatra–Andaman sequence is consistent with their observation in addition to extending it up to $M_0 \sim 10^{22}$ N m. The acceleration spectra for the earthquakes in this study, in which M_W ranged from 6.0 to 9.1, are plotted in Figure 9. Moderate-size earthquakes with M_W below 7.0 exhibit Brune-type spectra in which spectral amplitudes increase as ω^2 at low frequencies and are approximately flat above the corner frequency. As M_W increases, especially above M_W 7.0, the transition in the spectra between the ω^2 spectra at low frequencies and the flat spectra at high frequencies becomes noticeably wider and smoother. The marked change in spectral shape indicates that the slip in large earthquakes continues for a significantly longer duration that the slip in moderate earthquakes. Boatwright and Choy (1989) interpret the abrupt change in spectral behavior by the large and great earthquakes as resulting from rupture of the entire seismogenic width, with duration increasing as slip continues along strike.

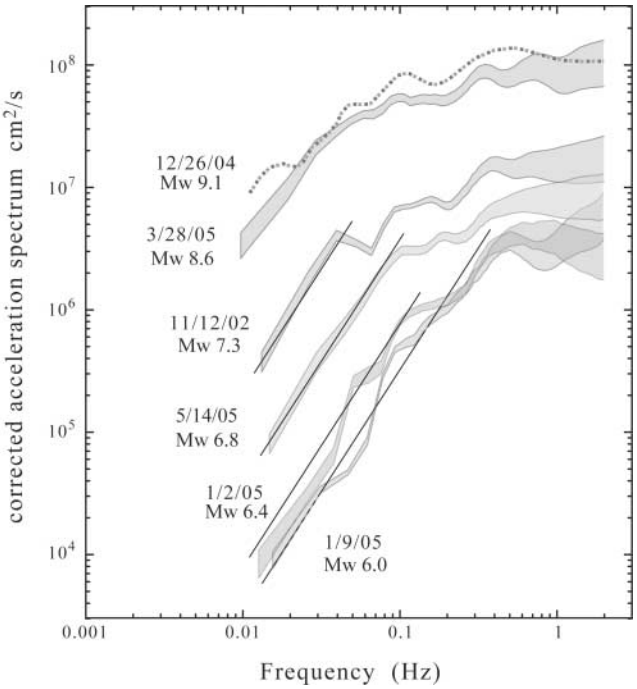

Figure 9. The corrected acceleration spectra of the five Sumatra events. As M_W increases the sharpness of the transition between the high- and low-frequency asymptotes decreases. Solid lines are ω^2 fits to the low-frequency spectra of the moderate-sized and transitional earthquakes with M_0 less than about 10^{20} N m. For earthquakes with M_0 greater than about 10^{20} N m, the ω^2 line falls below the frequency band of our spectral windows.

Conclusions

We have derived a procedure to estimate the seismic energy radiated by the 26 December 2004 Sumatra–Andaman earthquake. From four reference events with magnitudes ranging from 6.2 to 8.6, we determined a frequency-dependent correction operator that accounts for the arrival of secondary phases in the extended (~10-min) windows. This analysis is checked by predicting the source spectra for the shorter window by applying the correction operator to the source spectra of the extended window. While there is some variability for the three smaller earthquakes, the method predicts the source spectra of the 28 March 2005 earthquake very well. From the corrected-source spectrum of the Sumatra–Andaman mainshock we derive an E_S of 1.4×10^{17} J. From relative differences in the spectrum of the corrected ~600-sec window and the short ~250-sec window, we infer that the second half of the rupture, which radiated less high-frequency energy (between 0.07 to 0.7 Hz), is fundamentally different than the rupture process in the first half.

Acknowledgments

The authors are grateful to James W. Dewey, Charles Bufe, Anupama Venkataraman, and Andrew Newman for careful reviews of the manuscript. The authors benefited from discussions with Shri Singh, Hong-Kie Thio, and Hiroo Kanamori.

References

Ammon, C. J., C. Ji, H.-K. Thio, D. Robinson, S. Ni, H. Kanamori, T. Lay, S. Das, D. Helmberger, V. Hjorleifsdottir, G. Ichinose, J. Polet, and D. Wald (2005). Rupture process of the 2004 Sumatra–Andaman earthquake, *Science* **308,** 1133–1139.

Bilham, R. (2005). A flying start, then a slow slip, *Science* **308,** 1126–1127.

Boatwright, J., and G. L. Choy (1986). Teleseismic estimates of the energy radiated by shallow earthquakes, *J. Geophys. Res.* **91,** 2095–2112.

Boatwright, J., and G. L. Choy (1989). Acceleration source for subduction zone earthquakes, *J. Geophys. Res.* **94,** 15,541–15,553.

Choy, G. L., and J. L. Boatwright (1995). Global patterns of radiated seismic energy and apparent stress, *J. Geophys. Res.* **100,** 18,205–18,228.

Choy, G. L., and V. F. Cormier (1986). Direct measurement of the mantle attenuation operator from broadband P and S Waveforms, *J. Geophys. Res.* **91,** 7326–7342.

Harvey, D., and G. L. Choy (1982). Broadband deconvolution of GDSN data, *Geophys. J. R. Astr. Soc.* **69,** 659–668.

Houston, H. (1990). Broadband source spectra, seismic energies, and stress drops of the 1989 Macquarie Ridge earthquake, *Geophys. Res. Lett.* **17,** 1021–1024.

Ishii, M., P. M. Shearer, H. Houston, and J. E. Vidale (2005). Extent, duration and speed of the 2004 Sumatra–Andaman earthquake imaged by the Hi-Net array, *Nature* **435,** 933–936.

Kanamori, H. (2006). The radiated energy of the 2004 Sumatra–Andaman earthquake, in *Radiated Energy and the Physics of Earthquake Faulting*, R. Abercrombie, A. McGarr, H. Kanamori, and G. Di Toro (Editors), American Geophysical Monograph (in press).

Krüger, F., and M. Ohrnberger (2005). Tracking the rupture of the M_w = 9.3 Sumatra earthquake over 1,150 km at teleseismic distance, *Nature* **435,** 937–939.

Lay, T., H. Kanamori, C. J. Ammon, M. Nettles, R. Aster, S. L. Beck, S. Bilek, M. R. Brudzinski, R. Butler, H. R. DeShon, G. Ekström, K. Satake, S. Sipkin, and S. N. Ward (2005). The great Sumatra–Andaman earthquake of 26 December 2004, *Science* **308,** 1127–1133.

Lomax, A. (2005). Rapid estimation of rupture extent for large earthquakes: application to the 2004, M 9.0 Sumatra–Andaman megathrust, *Geophys. Res. Lett.* **32,** L10314, doi 10.1029/2005GL022437.

Newman, A. V., and E. A. Okal (1998). Teleseismic estimates of radiated seismic energy: the E/M_0 discriminant for tsunami earthquakes, *J. Geophys. Res.* **103,** 26,885–26,898.

Perez-Campos, X., and G. Beroza (2001). Is there a focal mechanism dependence to radiated seismic energy? *J. Geophys. Res.* **106,** 11,127–11,136.

Singh, S. (2005). Source spectrum and radiated energy from the Great Sumatra Earthquakes of December 26, 2004 and March 28, 2005, in *Abstracts of the AGU Chapman Conference on Radiated Energy and the Physics of Earthquake Faulting*, American Geophysical Union, Washington, D.C., p. 14.

Venkataraman, A, and H. Kanamori (2004). Observational constraints on the fracture energy of subduction zone earthquakes, *J. Geophys. Res.* **109,** B05302, doi 10.1029/2003JB002549.

U.S. Geological Survey
Box 25046, MS 966
Denver Federal Center
Denver, Colorado 80225
(G.L.C.)

U.S. Geological Survey
Menlo Park, California 94025
(J.B.)

Manuscript received 18 January 2006.